

Reusable piezo-sandwiched PTFE film for in-process monitoring of advanced composites

Elie Mahfoud  and Mohammad Harb

Journal of Intelligent Material Systems and Structures

2021, Vol. 32(20) 2463–2476

© The Author(s) 2021

Article reuse guidelines:

sagepub.com/journals-permissions

DOI: 10.1177/1045389X211002660

journals.sagepub.com/home/jim



Abstract

Environmental and cost-saving advantages derived from the use of composites attract aerospace and automotive industries as these materials offer significant structural and aerodynamic advantages over traditional metal structures. The composites industry, however, is concerned with the manufacturing processes as they cannot provide fast enough cycle time to match metal alloy processes. Our research aims to develop a sensing technology in the form of a reusable in situ cure monitoring and assessment system that can predict the formation of manufacturing defects and monitor the degree of cure. Thin-film material is chosen from various PTFE-based material by prioritizing the debonding effect and signal transmission through the composite part. Then, the film is used to sandwich piezoelectric actuators and sensors to monitor out-of-autoclave carbon fiber composite plates using ultrasonic Lamb waves by temporarily adhering to the manufactured part creating an effective electromechanical coupling between the sensing film and the laminate. Initial results, through the analysis of the fundamental antisymmetric A_0 mode at low frequencies, indicate that analyzing the velocity and amplitude of these waves over cure time determines gelation and vitrification points. Experimental results have also proved the feasibility of using such a reusable film for different curing cycles, always determining certain cure parameters.

Keywords

Carbon fiber composites, cure behavior, process monitoring, non-destructive testing, ultrasonics, lamb waves

1. Introduction

The composites industry has been growing exponentially in the past two decades. According to Holmes (2019), the global market size of this industry reached 1.82 billion dollars at the beginning of 2019. This fast growth indicates that various companies are realizing the advantages of this material and are incorporating it in numerous applications from sports equipment to the aerospace industry. However, manufacturers still struggle with its production time as the curing cycles are often established based on trial and error and are not optimized to their highest potential (Lindrose, 1978). Another problem that the industry faces is the defects within the composites coming from high porosity levels during manufacturing. Porosity is the bulk of many micro-voids which are induced from wetness or trapped air that, when culminating together, reduce the mechanical properties of the cured composite (Birt and Smith, 2004). These problems require a system that can effectively monitor the composites in real-time during curing while tracking defects and/or damage inside the parts. Bekas et al. (2019) fabricated a multi-functional

sensor consisting of inkjet-printed silver-based circuits and interdigital sensors for the structural health monitoring of a bonded composites repair without weight addition. Whereas Scheerer et al. (2017) made a piezo-temperature sensor to be integrated in the manufacturing process of resin transfer moulding (RTM). The goal of this work is to develop such a system that monitors the composite laminates during traditional curing inside an oven while being reusable to lower the cost and material consumption.

Established resin cure monitoring methods such as dynamic mechanical analysis (DMA), differential scanning calorimetry (DSC), rheology, and dielectric analysis (DEA) are widely used but mostly limited to a lab

Laboratory of Smart Structures and Structural Integrity, Department of Mechanical Engineering, American University of Beirut, Beirut, Lebanon

Corresponding author:

Mohammad Harb, Laboratory of Smart Structures and Structural Integrity, Department of Mechanical Engineering, American University of Beirut, Riad El-Solh, Beirut 1107, Lebanon.
Email: mh243@aub.edu.lb

setup under ideal conditions and are not feasible to be used at an industrial production and processing level (Hardis et al., 2013). They are still important, however, as they provide high quality information about glass transition temperature (T_g), cure onsets, completion of cure, and degree of cure (Pang and Gillham, 1990). These methods also give several cure parameters in function of time such as minimum viscosity of the polymer, gelation (cross-linking), and vitrification (glassy state) points (Lange et al., 2000; Nixdorf and Busse, 2001). Stark et al. (2015) tested different carbon fiber samples using DMA under different heating rates, damping frequencies, and overall ramp cycle to study the dependency of the liquid, rubbery, and glassy states to these changes. On the other hand, research involving ultrasonic methods was also used to study the resin curing cycle. Challis et al. (2000) have shown that using compression and shear ultrasonic waves, the structure growth and cross-linking time of the resin can be determined. Aggelis and Paipetis (2012) monitored epoxy resin using bulk ultrasonic waves and identified the gelation and vitrification points respectively through amplitude curves and wave velocity curves using ultrasonic transducers. They showed that velocity is linked directly to the stiffness of the resin, while viscosity relates to the attenuation of the propagating wave. Lionetto and Maffezzoli (2013) used air-coupled transducers to determine the onsets of both gelation and vitrification where they found out that the second onset happens because the kinetics of the reaction slow down and the latter becomes diffusion controlled. Hudson and Yuan (2018) created an automated process to monitor the carbon fiber composite using guided Lamb waves. Their discoveries relied only on the amplitude graphs of the propagating Lamb waves to determine all three cure parameters.

Lamb waves, named after Horace Lamb (1917), are elastic waves present in thin solid media that propagate by reflecting off the upper and lower boundaries of the plate thus expanding into two sets of wave modes: symmetrical in-plane, and anti-symmetrical out-of-plane modes. They have been used in various nondestructive testing (NDT) applications to evaluate and monitor the structural properties and integrity of different metallic and non-metallic structures. Being reliably capable of propagating, highly sensitive to damage, and easily generated and collected, Lamb waves offer high-precision damage detection, making it a competitive substitute to traditional NDT tools (Su et al., 2006). Harb and Yuan (2015, 2016) assembled a fully non-contact system for identification of delamination in composite laminates using the fundamental antisymmetric (A_0) Lamb wave mode. The same research group used Lamb waves for imaging hardly visible damages in metallic and composite plates (Harb and Yuan, 2017). Mustapha et al. (2011) proposed a practical approach for the detection of debonding in sandwich composite structures using a

time-reversal technique based on A_0 Lamb wave mode at low frequency. Okabe et al. (2010) offered a new delamination detection method based on the change in the dispersion characteristic from the information obtained about the Lamb wave mode conversion using Macro-Fiber Composite (MFC) actuators and Fiber Bragg Grating (FBG) sensors on a quasi-isotropic CFRP laminate. Mehrabi and Soorgee (2019) employed Lamb waves to detect the curing of two adhesives. They identified the process in three stages: uncured, semi-cured, and fully-cured resin while having the amplitude of the wave dropping as the adhesive cures. More recently, guided Lamb waves have been used for more variant research such as: characterizing the friction stir welded joints of dissimilar materials using the frequency-wavenumber filtering technique (Fakih et al., 2017), optimizing sensor placement on metallic and composite structures for maximum damage detection coverage area having minimum number of PZTs glued to the surface (Ismail et al., 2019), and determining the adhesion quality within three-layer structures (aluminum/adhesive/composite) which serves as a basis for future large scale manufacturing process quality control (Attar et al., 2020).

The focus of this paper is to (a) investigate the proper material needed to design and fabricate such system, (b) examine the use of ultrasonics to monitor the curing cycle through certain wave parameters, and (c) study the feasibility of this monitoring process. A reusable flexible sensing film promotes recycling and induces less wasted material while being faster for monitoring purposes. The material selection for this sensing film would be based on chemical, electrical, and mechanical properties. Among several material candidates that possess the required properties such as high melting temperature, matching acoustic impedance, and chemical inertness, Polytetrafluoroethylene (PTFE) commonly known as Teflon is a good candidate. Teflon has been used as artificial delamination in-between layers for composite testing (Cahain et al., 2014; Deng, 1995) which allows debonding to happen easily by separating the inserted film from the composite. Moreover, PTFE is used as fiber filler for the thermoplastic polymer Polyetheretherketone (PEEK) to fabricate a composite with lower friction coefficient and higher resistance to wear than the virgin PEEK material (Vail et al., 2011). Another test showed that the lowest shear stress, lowest breakdown time, and highest contact angle were observed in the PTFE barrier-epoxy resin combination in comparison to other material (Vogelsang et al., 2002). In addition, PTFE is known for its liquid repellency as it shows hydro- and oleo-phobic properties especially in the kitchenware industry (Coulson et al., 2000). Such properties make it an ideal candidate to be used as the required thin film.

This paper first introduces the experimental work in selecting the thin film material by making sure it

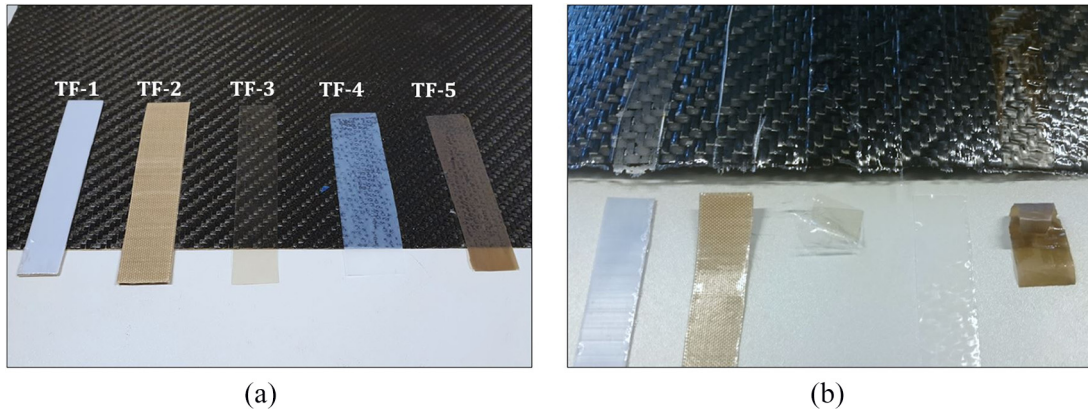


Figure 1. Thin film specimens: (a) before and (b) after peel test.

Table 1. Thin film material used and peeling test results.

Specimen	Material	Film thickness (mm)	Peel test
TF-1	Skived PTFE	0.5	No bond
TF-2	Glass cloth PTFE	0.25	No bond
TF-3	FEP	0.13	Bonded
TF-4	Cast PTFE	0.25	No bond
TF-5	TFM	0.08	Bonded

debonds from the carbon fiber after curing and transmits readable Lamb wave signals throughout the material. Then, this work reports on the online monitoring of unidirectional and woven laminates, the effect of the thin film on the generated Lamb wave modes and provide several trend line analysis discussing cure parameters using the proposed system. Eventually, the feasibility of this reusable sensing film is verified by tracking down the same cure parameters on a different curing cycle.

2. Material selection

2.1. Bonding test

Samples of five different materials shown in Table 1, consisting of three PTFE films, one modified PTFE (TFM), and one Fluorinated ethylene propylene (FEP), are investigated for bonding strength and ultrasonic signal transmission. These materials have acoustic impedances close to that of epoxy with low electrical dissipation factor and possess chemical inertness. Long strips ($15 \times 80 \text{ mm}^2$) were cut from each material and placed directly on the top of an uncured carbon fiber laminate, as shown in sure 1(a), which was then cured under vacuum following the manufacturer's curing cycle. After curing, the strips were manually peeled off the sample to study the bonding of the material with the laminate post curing. The peeled samples as seen in

Figure 1(b) show that TFM and FEP partially bonded to the plate while the three PTFE samples peeled off easily leaving a smooth surface finish on the plate.

2.2. Signal transmission

The non-bonded materials from the previous test were further investigated for their wave propagation effectiveness when sandwiching an ultrasonic transducer. The emphasis of this experiment is on the amplitude of the excited and received signals through the different PTFE materials. A $300 \times 300 \times 3 \text{ mm}^3$ Aluminum (Al-1050) plate was used as the base structure with five disc-shaped piezoceramic transducers (PZTs), 1 mm thick \times 10 mm in diameter, glued directly on the plate and three other discs were placed inside $30 \times 15 \text{ mm}^2$ sandwich of each PTFE material as illustrated in Figure 2. The PTFE sandwiched PZTs were not glued to the Aluminum plate but were assumed to have a near perfect adhesion when the whole sample is under vacuum.

Five-peak sinusoidal Hanning-windowed signal, generated by a Keysight 33500B signal generator and amplified by an EPA-104 Piezo System Inc amplifier, was used to excite PZTs. On the other end, sensing PZTs were recording any measured signal via a Keysight InfiniiVision DSO-X 3024A oscilloscope. The actuators and the sensors are 150 mm apart which is enough distance for the two Lamb wave modes, symmetric S_0 and antisymmetric A_0 , to be separated discretely for the selected frequency of 250 kHz. Two main studies were carried out such that the PZTs sandwiched with the PTFE materials were either actuators or sensors. This is because excitation and reception of the signal with the addition of the PTFE layer on only one side is not reversible. The reflections within the PTFE boundaries would differ hence resulting in a difference in the sensed signal. Then, each of the two studies had three different cases depending on the propagation direction of the wave or actuator-sensor combination. For instance, S4B4, S4B3, S4B2 would be respectively

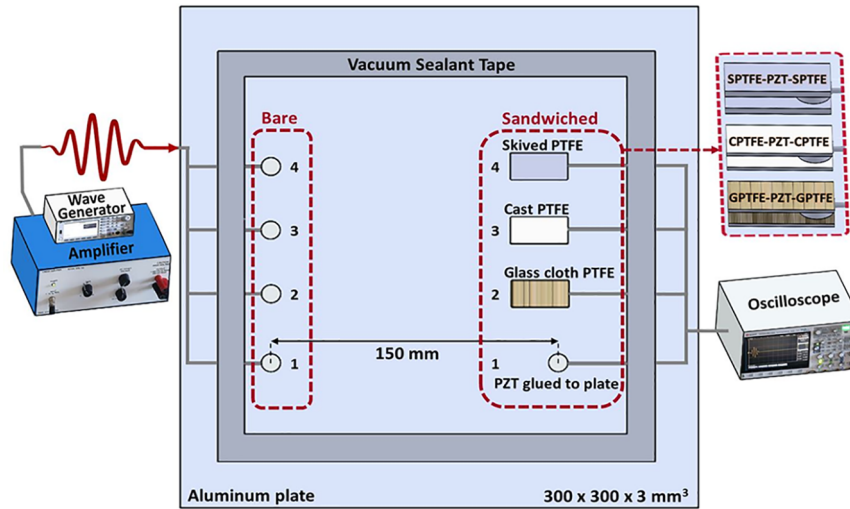


Figure 2. Experimental setup for signal intensity measurement using sandwiched PZTs (not drawn to scale).

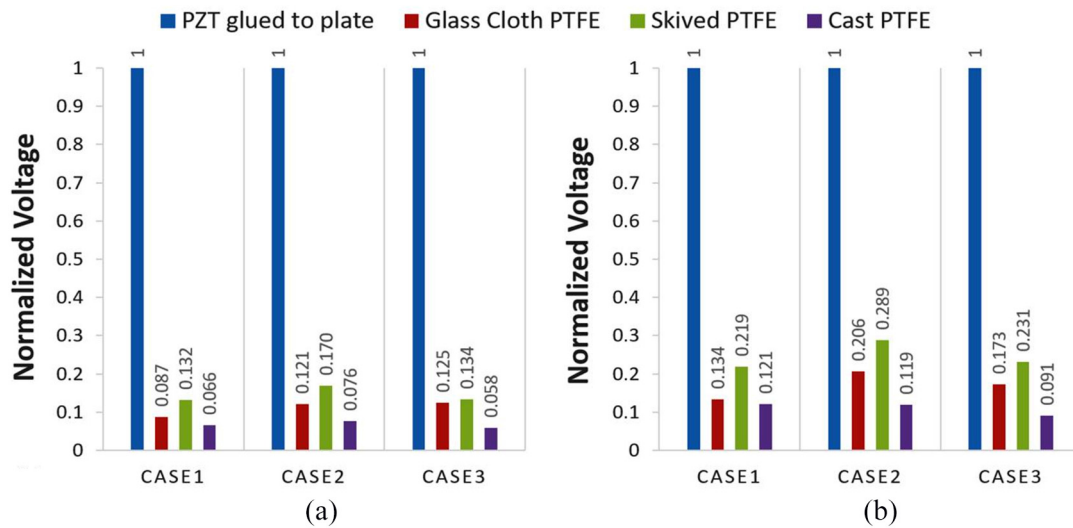


Figure 3. Normalized amplitude for S_0 mode at 250 kHz for the different materials in all three cases where sandwiched PZTs act as (a) actuators and (b) sensors.

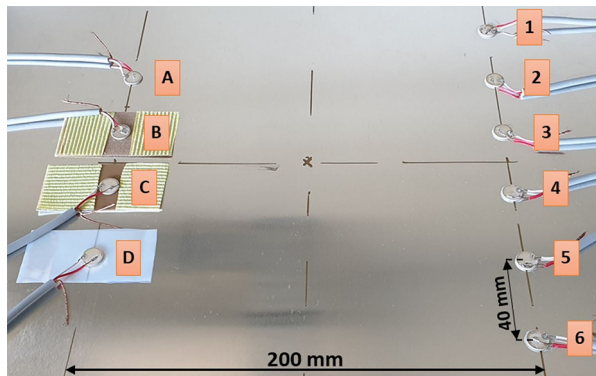
case 1, case 2, and case 3 for the first study when the Skived PTFE sandwiched (S) PZT is an actuator and the bare (B) PZTs are sensors; whereas B4S4, B3S4, and B2S4 would be the same cases respectively for the second study when the bare PZTs are actuators and Skived PTFE sandwiched PZT acts as a sensor. In both studies the obtained data are compared to the baseline data measured from S1B1, S1B2, S1B3 or B1S1, B2S1, B3S1.

For the used frequency of 250 kHz, the S_0 mode is dominant over A_0 in aluminium according to the tuning curves from both theory and experiments (Malaeb et al., 2018). The amplitude of the highest peak of the

first received S_0 packet in the measured signal is compared for all PTFE sandwiched PZTs to check for the highest transmission among them. The results in Figure 3 for all six cases show that Skived PTFE has the best signal transmission compared to Cast and Glass cloth PTFE. The out-of-planar nature of the A_0 mode should make it spread through the added PTFE material in a higher relative amplitude than S_0 , which vibrates in the plane of the propagation direction, unlike A_0 which pulsates perpendicularly, that is, in the z -direction, to the wave moving direction. This is why the A_0 mode needs to be analyzed through these material too. The plate used is considerably small and the

Table 2. Number of cases recording highest amplitude for S_0 and A_0 Lamb wave mode at 100 and 200 kHz for different thin film materials.

	100 kHz		200 kHz		Total	%	Dominant modes	%
	S_0	A_0	S_0	A_0				
Glass cloth PTFE	0	0	2	2	4	25	2	25
Skived PTFE	0	4	2	1	7	43.75	6	75
Cast PTFE	4	0	0	1	5	31.25	0	0
Number of cases	4	4	4	4	16	100	8	100

**Figure 4.** Second signal transmission setup at the center of a $1000 \times 1000 \text{ mm}^2$ Al-1050 plate.

B is glass cloth PTFE, C is skived PTFE, and D is cast PTFE.

edge reflections coming from S_0 may coincide with the first received A_0 packet. Hence, another experiment with a bigger plate is conducted.

To better analyze the signal performance along the added PTFE, the signal generation was investigated over other frequencies where A_0 or S_0 are dominant. In Al-1050, according to the same theoretical and experimental tuning curves, the A_0 mode is dominant at 100 kHz while S_0 is the major mode at 200 kHz. It is worth mentioning that these experiments are in line with theory and with Giurgiutiu's (2005) work on this. Figure 4 shows the setup of the second wave generation experiment which was carried out in the center of a large $1000 \times 1000 \times 3 \text{ mm}^3$ plate to delay unwanted boundary edge reflections. One layer of each PTFE material with a cross-sectional area of $30 \times 60 \text{ mm}^2$ is placed underneath transducers B, C, and D. Vacuum was always used to enhance contact. Two additional PZTs, 1 and 6, were also glued on the right side making one more additional path for each material, thus a fourth case. The materials were only used as actuators for four cases and tested with the two frequencies. Figure 5 shows the horizontal path case of signal generation (A2, B3, C4, and D5 from Figure 4) where it is clear that the two modes are separated, and no reflections overlap with the first received A_0 packet. It is noticeable how the weaker S_0 mode at 100 kHz is barely recorded by the PZTs layered over the PTFE

materials. In fact, although S_0 is dominant at 200 kHz, its amplitude is still read lower than A_0 by these PZTs. Table 2 summarizes the results of all 16 studied cases where for each frequency, exist 4 cases for each mode. The table also demonstrates the eight dominant mode cases: A_0 at 100 kHz and S_0 at 200 kHz.

Unlike the first signal transmission experiment, Skived PTFE does not have the highest amplitude in all cases. For the dominant A_0 mode at 100 kHz and the dominant S_0 mode at 200 kHz, Skived PTFE leads with all four cases and two cases (shared Glass cloth PTFE), respectively. For the weaker S_0 mode at 100 kHz and A_0 mode at 200 kHz, Cast and Glass cloth PTFE have the highest amplitudes, respectively. For the sum of all cases, Skived PTFE transmits the highest amplitudes in 7 out of 16 cases while it leads in 6 out of 8 dominant mode cases. Knowing that this material has a 0.5 mm thickness while the Cast and Glass cloth PTFE were both 0.25 mm thick, Skived PTFE was clearly chosen to be the sole candidate for the cure monitoring application.

3. Cure cycle monitoring

3.1. Experimental setup

Two kinds of composite laminates were considered in this study for the cure monitoring experiments. The first is an autoclavable XPREG XC130 unidirectional Pre-impregnated Carbon Fiber-Reinforced Polymer (CFRP) and the second is an out-of-autoclave XPREG XC110 woven prepreg CFRP. In this work, both composites were cured in a precision composites curing oven (OV301 *easycomposites*TM) under vacuum and heat. In the absence of an autoclave, the manufacturer suggested using the same out-of-autoclave cycle for both types. While the parts were under vacuum, the heating cycle started at room temperature and heated slowly at a rate $1^\circ\text{C}/\text{min}$ until it reached 70°C and left soaking at that temperature for 4 h. The oven was then heated to 120°C at a $2^\circ\text{C}/\text{min}$ heating rate and soaked for 1 h and then cooled down to room temperature naturally. Figure 6 shows this curing cycle including both heat and pressure.

Two separate cure monitoring experiments were done during this study. The first cure monitoring

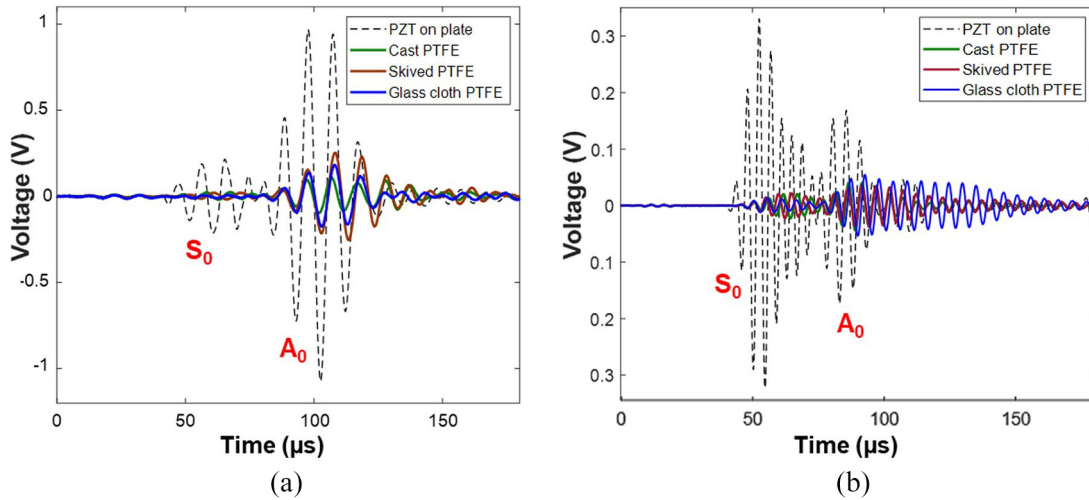


Figure 5. Sensed signals by the bare PZTs when actuated from the sandwiched ones with excitation frequencies of (a) 100 kHz and (b) 200 kHz.

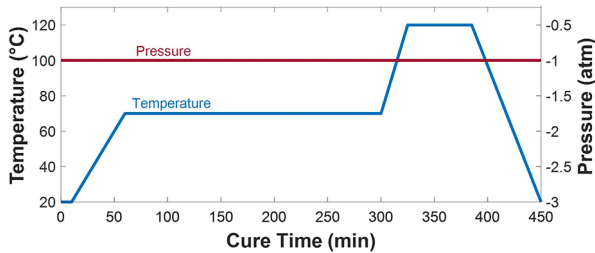


Figure 6. Cure cycle of the out-of-autoclave prepreg as proposed by the manufacturer.

experiment was done on two unidirectional $[0]_3$ CFRP laminates while the second was investigated on two woven $[0/90/0]$ CFRP laminates. All laminates were $220 \times 350 \times 1 \text{ mm}^3$ in dimensions. Figure 7 shows the setup of this experiment where a $700 \times 400 \times 6 \text{ mm}^3$ aluminum plate is used as the tooling plate. The plate is partitioned into three equal sections. Section A has an actuating and sensing PZT directly glued on the aluminum which will monitor any change involving the PZTs and Al plate during the curing cycle for any temperature effect. Section B holds one CFRP laminate with PZT sensor and actuator directly placed on its top surface. Section C holds another CFRP laminate with PZT sensor and actuator sandwiched between two Skived PTFE films over the composite. The Skived PTFE films were 0.5 mm thick each, of the same size as the CFRP plate and with adhesive silicone layers on one side which were cut and joint together having two PZTs in between. All PZTs used were disc shaped PZT-5J material type with 0.5 mm thickness, 7 mm diameter, and had 320°C Curie temperature making them effective for temperatures up to 160°C as recommended by the manufacturer. The PZT wires are soldered below Curie temperature using 60-40% Sn-Pb

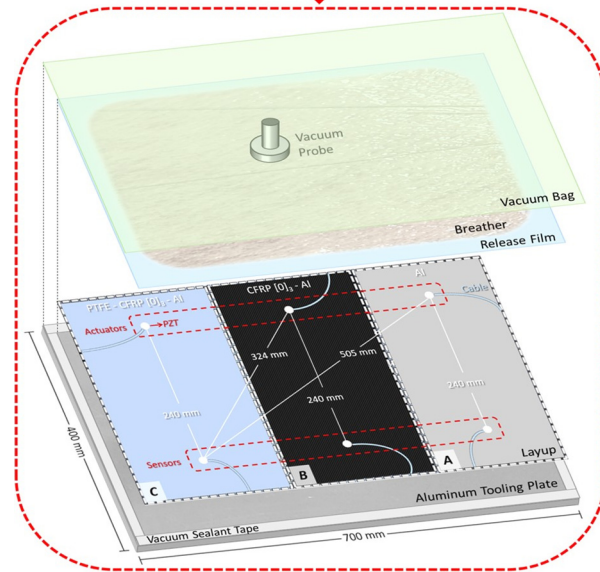
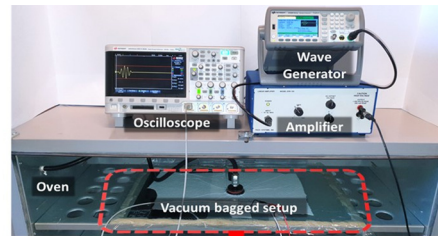


Figure 7. First cure monitoring experiment setup showing different paths that are tracked for each actuator-sensor.

solder that has a 190°C melting temperature. Silicone release agent was sprayed on the Al plate under the two CFRP plates to prevent any bonding. The plate was then placed in a vacuum bag with the wires well sealed to prevent air leak during vacuum and then placed in an oven following the manufacturer’s recommended curing cycle.

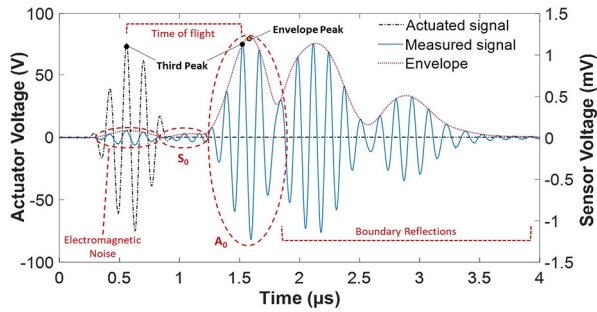


Figure 8. Measured signal from the PTFE sandwiched actuator-sensor film at 10 min into the curing cycle.

The actuation and sensing system used in the earlier experiment was also implemented in this experiment. The amplified signal to the actuator was 160 V_{pp} (peak-to-peak voltage) at a central frequency of 70 kHz. This frequency was chosen after some testing as it provides the highest A_0 amplitude and nearly eliminates S_0 in the unidirectional CFRP. This does not apply to the woven CFRP as both modes are very clear in this prepreg, but we kept the same frequency for the purpose of comparison. Data was being measured by the oscilloscope every 10 min from all three sensors in sections A, B, and C for each actuator.

3.2. Results

The data collected is analyzed through two parameters: the voltage of the received signal and the group velocities of the generated modes. The group velocity is simply the distance between the transmitting and receiving transducers, covered by the propagating signal, divided by the time-of-flight. When the Lamb wave propagates through any material, depending on its properties and the excitation frequency, the excited signal inherits dispersion. This means that the number of peaks in a packet can increase as it travels, and the amplitude of the highest peak decreases as it shifts from the third peak in the input signal to other peaks at the centroid of the sensed signal, which causes slower moving packets as the time between the third peak of the actuator and the centroid of a dispersive wave would increase. This phenomenon is mentioned because while dealing with this data, some signal paths caused the waves to be slightly dispersive causing the analysis to take on two forms: through the signal itself and its envelope. If dispersive, the envelope's highest point would be the centroid, giving the actual group velocity, and the third peak, which is now ahead of the centroid, would give a velocity in between the phase velocity and the group velocity. For simplicity, both are called group velocities and the better trend of the two is chosen. Figure 8 shows an example of a measured signal from the PTFE sensing film over the unidirectional composite.

For the same sensing film and CFRP, Figure 9 shows data points of group velocity and voltage as a function of curing time. It also shows the difference between using the third peak and the envelope to calculate these parameters. While the voltage curves show the same trend with minor differences in the values at the beginning and end of the cycle, the velocity curves are similar except for the obvious shift in the middle 4-h soak section as the envelope goes faster by almost 100 m/s during this liquid phase. For most of the paths analyzed, the group velocity curves are better evaluated when using the third peak instead of the moving envelope peak. Thus, in this work, velocity and voltage curves are measured according to the signal's third peak. Future plots will show only the trends of the curves without inclusion of the data points for better visuals.

3.2.1. Trendline analysis and comparison. Figure 10 shows the group velocity and signal amplitude curves for the A_0 Lamb wave mode for seven paths from the first cure monitoring experiment in Figure 7. Starting with the bare aluminum path plotted in dark red ($AL_{act} - AL_{sen}$) in Figure 10(a) and (b), its velocity and voltage slightly decrease with the increase in temperature. This could be explained by the almost linear decrease of the elastic modulus of aluminum during the curing cycle due to the increase in temperature (Gerlich and Fisher, 1969) which the velocity and attenuation of Lamb wave depend on. With such insignificant change in velocity and voltage compared to the other curves, mainly those of the $PTFE_{act} - PTFE_{sen}$ and $UNI_{act} - UNI_{sen}$ paths, it is feasible to assume that the propagation of Lamb wave in aluminum during the curing cycle stays intact. Notice that at 450 min, the ($AL_{act} - AL_{sen}$) path velocity and voltage curves still haven't gone back to their initial values. This is because the plate temperature after only 1 h of natural cooling is still in the 50°C–60°C range and haven't reached room temperature yet. Once it did after 2–3 h, both the velocity and voltage went back to their initial state.

On the other hand, the setup is under vacuum during the cure cycle which would create a near perfect bond between the aluminium and the composite laminates. Thus, the effect of this bond creating a CFRP-Aluminium composite in section B and PTFE-CFRP-Aluminium composite in section A on the generated Lamb wave needs further investigation. The velocity and voltage curves for all other paths, as seen in Figure 10, drop at the beginning of the cure cycle due to the consolidation of the prepreg and then becoming a viscous fluid with a plateaued curve until it reached a drop when it starts the gelation process which then increases and stabilizes when it solidifies. It is noticed that the group velocities of all six paths passing through the composite plates are lower than the group

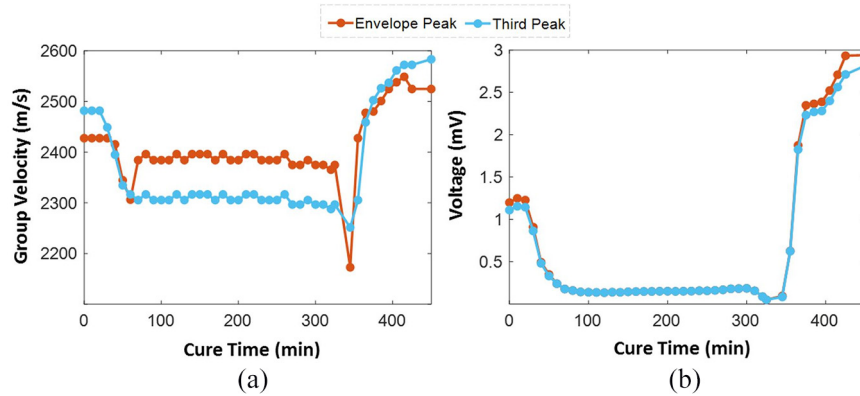


Figure 9. (a) Group velocity and (b) voltage of A_0 mode generated and received by the skived PTFE sandwiched PZTs over the $[0]_3$ unidirectional laminate.

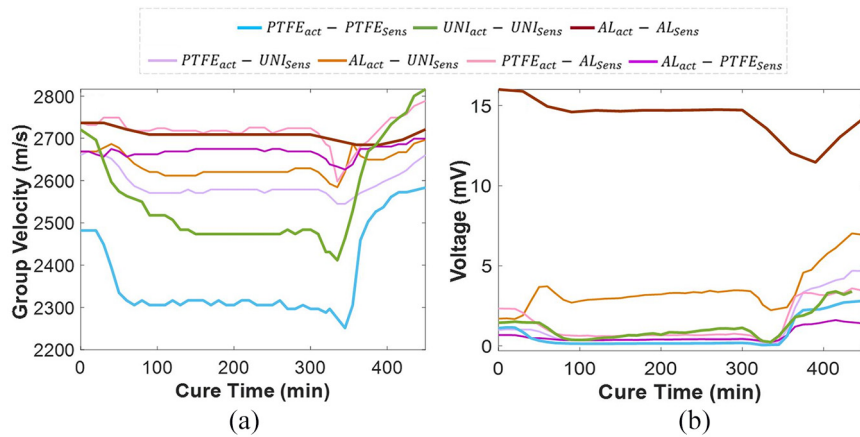


Figure 10. (a) Group velocity and (b) voltage of A_0 mode generated and received along different paths in the first cure monitoring experiment.

velocity from the $AL_{act} - AL_{sen}$ due to the interference of the wave with the laminates which have lower A_0 group velocity than the aluminium plate. That velocity is even much lower for the propagating wave within the same laminate: $PTFE_{act} - PTFE_{sen}$ and $UNI_{act} - UNI_{sen}$. Thus, the aluminium base plate does influence the group velocity of the A_0 mode since the laminates are in contact with the tooling plate due to vacuum and the silicone release agent. But since the monitored parameters are stable throughout the cure cycle as proven, we could assume that the measured data is viable to monitor the cure of a laminate.

Comparing directly the A_0 mode group velocity curves for unidirectional CFRP with and without the use of thin PTFE film in Figure 11(a) and (b), one can see that the velocity of A_0 shifts downwards when having PTFE due to the additional stacking in the PTFE-CFRP-Aluminum laminate under vacuum. However, the trends of the two velocity curves are very similar having a decrease in the velocity from 0 min to 100 min due to the initiation of resin consolidation inside the

prepreg. The resin becomes a viscous fluid with a relatively constant velocity between 100 min and 300 min until it reaches a drop when it starts the gelation process at 310 min. The minima after that indicates full gelation and then both curves increase until reaching an asymptotic value at the end of the cure. But before that, the trend of the incline changes halfway slowing the rate of cure and indicating an onset that Lionetto and Maffezzoli (2013) claimed to be the vitrification point which demonstrates the start of the glassy solid state.

The voltage curves show the same trend as the velocity curves except for a clear increase in the amplitude for the plate without PTFE during the liquid phase until it reaches a maximum around 300 min before dropping off. This maximum is also present in the PTFE path when zooming in on the curve. This, according to Hudson and Yuan (2018), represents the minimum viscosity of the resin before gelation, hence the latter starting after this point occurs. It is of interest to highlight the fact that this maximum occurs around

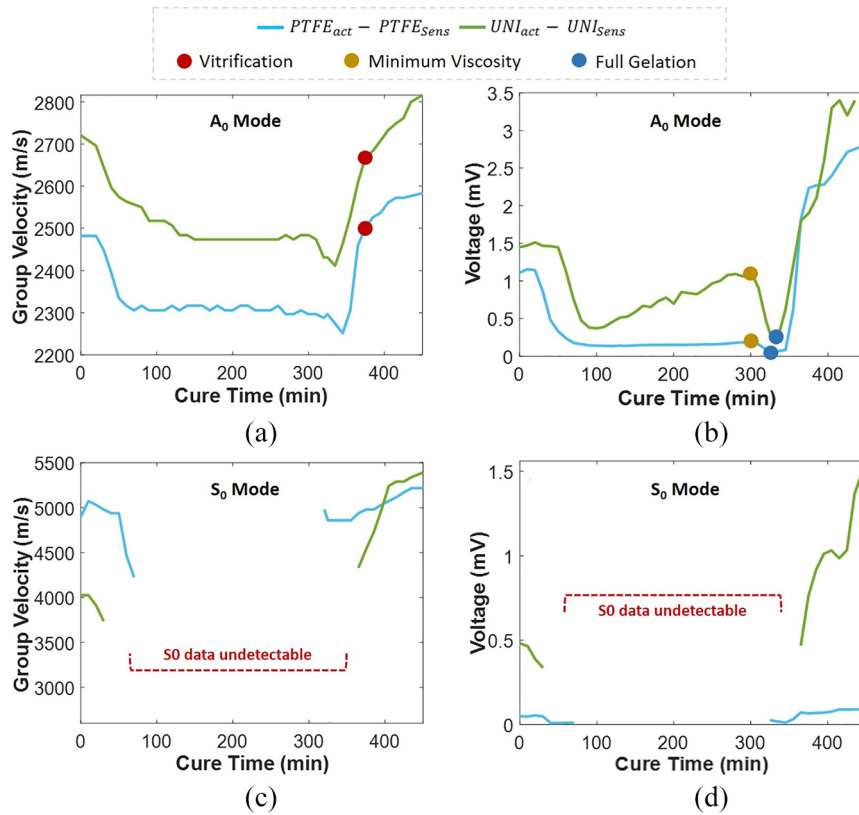


Figure 11. (a) Group velocity of A_0 mode, (b) voltage of A_0 mode, (c) group velocity of S_0 mode, and (d) voltage of S_0 mode generated and received over the $[0]_3$ unidirectional laminate.

the end of the first soak and the start of the second ramp in the cycle. Gelation is a process where the rubbery state is present in the prepreg after an irreversible transformation in the resin from liquid to gel due to the appearance of a cross-linked network and approaching infinite molecular weight (Prime, 1970). It takes place between the previous maximum (“minimum viscosity”) and the time of the previously discussed vitrification onset. The minimum point between the two indicates full gelation of the prepreg. Both $PTFE_{act} - PTFE_{sen}$ and $UNI_{act} - UNI_{sen}$ paths have the same times for minimum viscosity at 300 min, gelation at 335 min, and vitrification point at 375 min. A few minutes difference is noticed when these points were detected on the velocity and voltage curves. Hence, the first two parameters are always taken from the voltage curves while vitrification is acquired from the velocity curves as it is noticed in previous work. The velocity and voltage curves of S_0 mode plotted in Figure 11(c) and (d) show the absence of S_0 during the liquid stage for the $PTFE_{act} - PTFE_{sen}$ and $UNI_{act} - UNI_{sen}$ paths. The advantage of the $PTFE_{act} - PTFE_{sen}$ path is clearly visible as S_0 appears at the gelation point unlike the $UNI_{act} - UNI_{sen}$ path for which it appears at or just before vitrification. This indicates that monitoring the cure with frequencies where A_0 is dominant is a more reliable method because

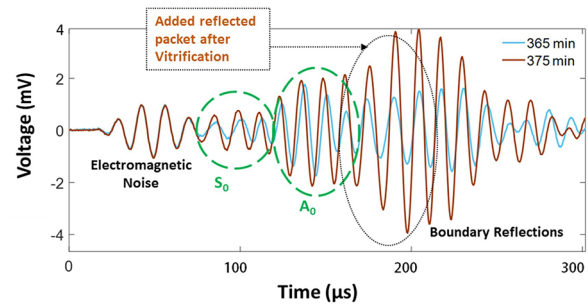


Figure 12. Raw data points from the $UNI_{act} - UNI_{sen}$ path showing the wave behavior before and after vitrification.

its out-of-planar nature allows it to pass through the several layers included in this bagging and monitoring process at all states of the prepreg as proven.

To further investigate the onset of vitrification of the unidirectional composite which occurred at 375 min, two raw signals from the $UNI_{act} - UNI_{sen}$ path taken at curing times 365 min and 375 min were plotted in Figure 12. It is noticed that right at the time of vitrification, the reflections have increased not only in amplitude but also in the number of peaks. This is noticed because after the part solidified, the plate’s boundary reflections and reflections from the nearly placed vacuum probe become more noticeable.

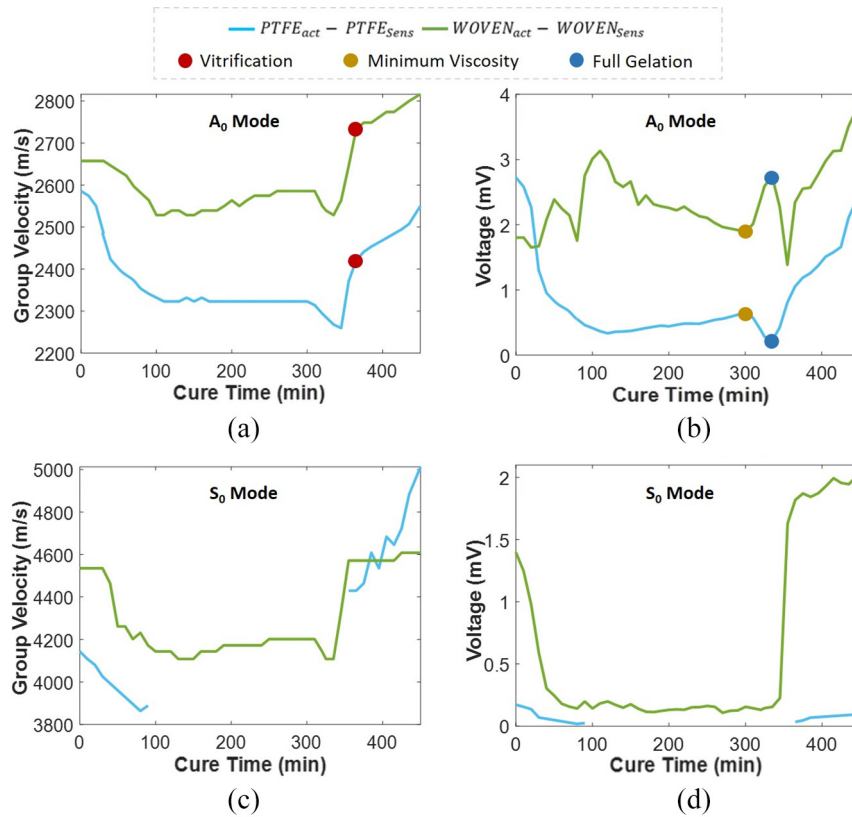


Figure 13. (a) Group velocity of A_0 mode, (b) voltage of A_0 mode, (c) group velocity of S_0 mode, and (d) voltage of S_0 mode generated and received over the $[0/90/0]$ woven laminate

The results for the cure monitoring of the woven CFRP in the second experiment are plotted in Figure 13. Almost similar trends to the curves from the previous experiment are noticed. However, the vitrification point for the woven laminate happens at 365 min rather than 375 min in the A_0 velocity plots. On the other hand, the A_0 amplitude curve for the $WOVEN_{act} - WOVEN_{sens}$ path seems distinct from the rest of the curves. The trend would be similar to its counterparts if the curve between 80 min and 345 min is flipped horizontally. It seems that the woven CFRP behaves differently than the unidirectional one during this time. This is especially interesting as the PTFE in this case seemed to have helped to identify the real trend. It is important to point out that the curves of the $PTFE_{act} - PTFE_{sens}$ path for both the unidirectional and woven laminates distinctly show the curing phases and the critical cure monitoring points. The S_0 mode in Figure 13(c) and (d) is shown even in the liquid state for the $WOVEN_{act} - WOVEN_{sens}$ path unlike the $UNI_{act} - UNI_{sens}$ before. While the vitrification onset is noticed in the velocity and voltage curves of the S_0 mode, the minimum viscosity and gelation points are only noticed in the velocity curve.

3.2.2. Post cure monitoring. Past curing and removal of the carbon fiber plates from the mold, data was

collected for the $UNI_{act} - UNI_{sens}$ and $WOVEN_{act} - WOVEN_{sens}$ paths to monitor the A_0 mode velocity strictly in the cured CFRP. The A_0 mode group velocities were measured at 1365 m/s for the woven CFRP and 1425 m/s for the unidirectional CFRP at 70 kHz, compared to 2830 m/s for the woven CFRP-Aluminum composite and 2816 m/s for the unidirectional CFRP-Aluminum composite. This affirms that when going through the monitored material, the wave was going inside the aluminum plate too creating a new laminate of both material making the wave faster due to the aluminum characteristics. This phenomenon enhances the cure monitoring since in the liquid stage of the resin, instead of the wave attenuating to degrees that cannot be measured, it is staying visible due to the presence of the aluminum while having the advantages of reading the changes inside the monitored part as seen in the different trendlines.

The two cured plates were placed once more in the same curing cycle and monitored for the second time after already reaching their final glassy state. This was done to check for the indifference in the signal that the $AL_{act} - AL_{sens}$ path showed previously. Figure 14 shows the group velocity and voltage curves of these two loose cured plates (woven and unidirectional), the previously discussed aluminum path and one more woven plate that is cured-to-bond with the aluminum plate underneath.

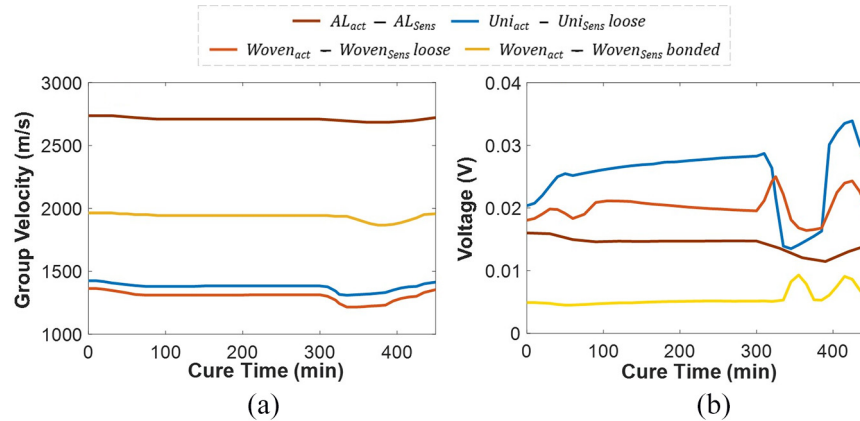


Figure 14. (a) Group velocity and (b) voltage of A_0 mode generated and received along different already-cured material.

The three new velocity curves show the same trend as the aluminum one but with slower speeds. Wang et al. (2015) mention that although fibers alone are temperature resistant in terms of mechanical properties, the resin matrix of the CFRP composite is “susceptible” to elevated temperatures thus making the composite rapidly lose strength and stiffness at elevated temperatures that are lower by 20°C or more than its T_g . The measured T_g from DMA experimentation for both unidirectional and woven cured CFRP plates are 110°C and 107°C respectively for T_g onset and 122°C and 118°C respectively for peak T_g (T_i). This shows in these velocity curves as they are losing velocity almost linearly during the two ramp stages indicating almost linear loss of elastic modulus. The two paths involving aluminum ($AL_{act} - AL_{sen}$ and $WOVEN_{act} - WOVEN_{sen}$ bonded) have a delayed decline in the group velocity or elastic modulus followed by an immediate incline (almost no constant velocity during the 120°C 1 h soak), unlike the two loose carbon plates that have constant velocity during this phase before an increase during the natural cooling stage. The thicker and larger aluminum plate takes more time to reach 120°C homogeneously than the loose thin CFRP plates. Thus, the relatively low values for the T_g onsets mentioned for the two materials above are understandable since they were previously semi-bonded to the Aluminum plate during their first cycle monitoring (during their cure).

The voltage curves on the other hand show that the curves of the two woven CFRP plates are distinct with an unusual trend after min 300 (start of second ramp). Unlike the decrease in voltage seen in $AL_{act} - AL_{sen}$ and $UNI_{act} - UNI_{sen}$ loose paths during this ramp, the two woven plates show an incline in voltage followed by a peak then a decrease leading to the regular trend that the other two curves present after the end of the second soak. This phenomenon present only in woven CFRP plates can be due to the different service temperatures set by the manufacturer to each XC130 and XC110 prepreg material (the difference is mainly in the epoxy

resin): the service temperature for the XC130 (unidirectional one) is 130°C while it is 115°C for the XC110 (woven one). When getting close to the service temperature of the woven CFRP plate and then exceeding it, the resin inside the plate can behave differently and react with the glue that is attached to the PZTs, hence the increase in the voltage during this time. Notice that in the $WOVEN_{act} - WOVEN_{sen}$ bonded voltage curve, this phenomenon is shifted to the right, this is explained by the previous velocity curve analysis: the shift is due to the aluminum taking longer to reach the program temperature. Just as discussed with the Aluminum plate case, the effect of the Lamb wave propagation in the CFRP cured plates is intact in terms of velocity but is not in terms of voltage. The voltage behavior is explained by both T_g and service temperature effects and is still distinct from the previous original cure monitoring analysis, hence the latter is still viable after this investigation. The next section will discuss the feasibility of trimming the cure cycle and monitoring it via the same proposed system.

4. Sensing feasibility of the proposed system

To validate the previous findings, a change in the curing cycle was made, especially since a reduction of the timeline required for the production and assessment of carbon fiber composites is needed in an industry where manufacturing processes do not provide fast enough cycle time to meet metal alloy processes. To test the possibility of trimming the cure cycle, another experiment is carried out involving the same XPREG XC110 woven carbon fiber prepreg. Very similar to Section C from the previous woven CFRP experiment, this “cycle time reduction” experiment involves the same layout and the same re-usable PTFE-PZTs sandwich sensing film.

The modification in the cycle should be in the longest soak period which is the 4 h soak at 70°C , especially since the cure parameters, as deduced earlier, were

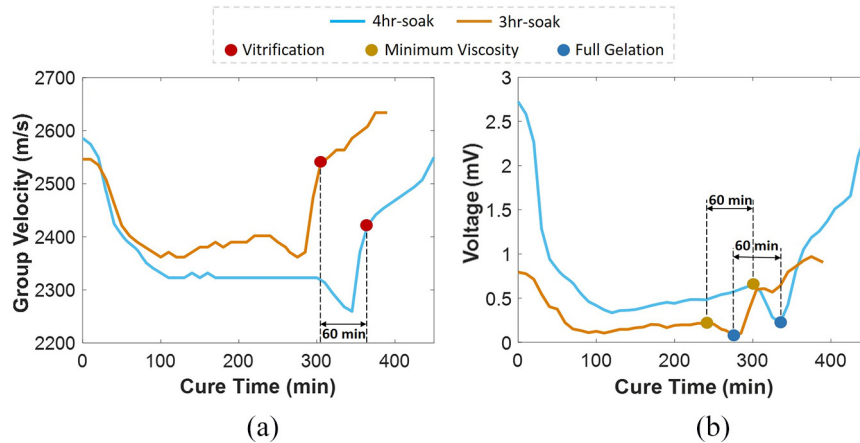


Figure 15. (a) Group velocity, and (b) voltage of A_0 mode generated and received over the [0/90/0] woven laminate for the 4 h-soak and 3 h-soak experiments

present in the second ramp and second soak stages following the end of this first (4 h) soak period. The aim is to reduce this soaking period by 1 h making the total time of the modified curing cycle 390 min instead of 450 min. The group velocity and voltage amplitude for the dominant A_0 mode for this 3 h soak experiment were analyzed and compared to the results of the previous experiment, as shown in Figure 15. Both curves follow the same trends, however, the 1 h shift between them is noticed after the first soak at 70°C is finished. The vitrification point is more reliably taken from the velocity curves while the minimum and maximum viscosity (gelation) points are better determined from the voltage curves. As seen, the three points are shifted exactly by 60 min earlier in the new experiment: vitrification moving from 365 min to 305 min, full gelation from 335 min to 275 min, and minimum viscosity (always at the end of the long soak) from 300 min to 240 min.

Although the trends of these curves shown are similar, the range of values differs slightly. The velocity curve in the new 3 h soak begins at a slightly lower value than its 4 h soak experiment velocity curve and then after 20 min, it surpasses the latter for the rest of the cycle. On the other hand, the amplitude of this A_0 mode in the 3 h soak experiment is always lower than that in the 4 h soak experiment. This could be due to a slight difference between the two experiments in either the layup, the amount of silicone release agent between the layup and the aluminum plate, or even the bonding between the sensing film and the layup. Besides these minor differences, the proposed system seems to function properly when monitoring the cure of the carbon fiber laminates regardless of the curing cycle tested.

5. Conclusion

In this paper, a reusable flexible thin film of PTFE material was viably used to monitor the curing cycle of two composites: unidirectional and woven pre-

impregnated CFRP laminates. First, the best material for the sensing film was chosen by eliminating candidates from both bonding and signal transmission experiments. Then, Skived PTFE was used as a sensing film by having sandwiched two disc-shaped PZTs inside. Using this film, identification of important curing parameters such as gelation and vitrification points was done through the analysis of the group velocity and the voltage curves of the generated fundamental Lamb wave modes (mainly the dominant mode A_0 at the used 70 kHz frequency) with the help of the aluminum plate placed below the laminates creating a bond during curing that allowed the monitoring during the liquid phase to be easier. After proving its reliability in terms of cure cycle monitoring, the film was used to monitor a trimmed cycle by 1 h for the woven prepreg and prove that the cure parameters stayed intact. Further studies are required to analyze the behavior of Lamb waves when PTFE layers are present on both sides of the composite plates separating it from the aluminum base plate. Also, more development can be made to further optimize the curing cycle by cutting down more time and enhance the composites industry by making the manufacturing process faster and reducing waste. The system will also be used in future work to monitor in real-time any induced manufacturing defects within the manufactured part while curing.

Acknowledgements

Recognition and gratitude are addressed to the University Research Board at the American University of Beirut and the Lebanese National Council for Scientific Research (CNRS).

Author contributions

Elie Mahfoud: Conceptualization, Formal analysis, Investigation, Writing—Original Draft, Visualization.

Mohammad Harb: Conceptualization, Validation, Writing—Review and Editing, Supervision, Funding acquisition.


Declaration of conflicting interests

The author(s) declared no potential conflicts of interest with respect to the research, authorship, and/or publication of this article.

Funding

The author(s) disclosed receipt of the following financial support for the research, authorship, and/or publication of this article: This work was supported by the University Research Board (URB) at the American University of Beirut [grant number 103371].

ORCID iD

Elie Mahfoud  <https://orcid.org/0000-0001-8239-4872>

References

- Aggelis D and Paipetis A (2012) Monitoring of resin curing and hardening by ultrasound. *Construction and Building Materials* 26(1): 755–760.
- Attar L, Leduc D, Kettani MECE, et al. (2020) Detection of the degraded interface in dissymmetrical glued structures using Lamb waves. *NDT & E International* 111: 102213.
- Bekas DG, Sharif-Khodaei Z and Aliabadi FMH (2019) A smart multi-functional printed sensor for monitoring curing and damage of composite repair patch. *Smart Materials and Structures* 28(8): 085029.
- Birt EA and Smith RA (2004) A review of NDE methods for porosity measurement in fibre-reinforced polymer composites. *Insight - Non-Destructive Testing and Condition Monitoring* 46(11): 681–686.
- Cahain YML, Noden J and Hallett SR (2014) Effect of insert material on artificial delamination performance in composite laminates. *Journal of Composite Materials* 49(21): 2589–2597.
- Challis R, Freemantle R, Cocker R, et al. (2000) Ultrasonic measurements related to evolution of structure in curing epoxy resins. *Plastics, Rubber and Composites* 29(3): 109–118.
- Coulson SR, Woodward I, Badyal JPS, et al. (2000) Super-repellent composite fluoropolymer surfaces. *The Journal of Physical Chemistry B* 104(37): 8836–8840.
- Deng X (1995) Mechanics of debonding and delamination in composites: Asymptotic studies. *Composites Engineering* 5(10–11): 1299–1315.
- Fakih MA, Tarraf J, Mustapha S, et al. (2017) Characterization of Lamb waves propagation behavior in friction stir welded joints of dissimilar materials. In: *The 11th international workshop on structural health monitoring (IWSHM)*, Stanford, California, 12–14 September 2017. Pennsylvania: DEStech Publications.
- Gerlich D and Fisher E (1969) The high temperature elastic moduli of aluminum. *Journal of Physics and Chemistry of Solids* 30(5): 1197–1205.
- Giurgiutiu V (2005) Tuned Lamb wave excitation and detection with piezoelectric wafer active sensors for structural health monitoring. *Journal of Intelligent Material Systems and Structures* 16(4): 291–305.
- Harb MS and Yuan FG (2015) Lamb wave dispersion and anisotropy profiling of composite plates via non-contact air-coupled and laser ultrasound. *AIP Conference Proceedings* 1650(1): 1229–1238.
- Harb MS and Yuan FG (2016) Non-contact ultrasonic technique for Lamb wave characterization in composite plates. *Ultrasonics* 64: 162–169.
- Harb MS and Yuan FG (2017) Barely visible impact damage imaging using non-contact air-coupled transducer/laser Doppler vibrometer system. *Structural Health Monitoring* 16(6): 663–673.
- Hardis R, Jessop JL, Peters FE, et al. (2013) Cure kinetics characterization and monitoring of an epoxy resin using DSC, Raman spectroscopy, and DEA. *Composites Part A: Applied Science and Manufacturing* 49: 100–108.
- Holmes M (2019) Additive manufacturing continues composites market growth. *Reinforced Plastics* 63(6): 296–301.
- Hudson TB and Yuan F-G (2018) Automated in-process cure monitoring of composite laminates using a guided wave-based system with high-temperature piezoelectric transducers. *Journal of Nondestructive Evaluation, Diagnostics and Prognostics of Engineering Systems* 1(2): 021008.
- Ismail Z, Mustapha S, Fakih MA, et al. (2019) Sensor placement optimization on complex and large metallic and composite structures. *Structural Health Monitoring* 19(1): 262–280.
- Lamb H (1917) On waves in an elastic plate. *Proceedings of the Royal Society of London. Series A, Containing Papers of a Mathematical and Physical Character* 93(648): 114–128.
- Lange J, Altmann N, Kelly C, et al. (2000) Understanding vitrification during cure of epoxy resins using dynamic scanning calorimetry and rheological techniques. *Polymer* 41(15): 5949–5955.
- Lindrose AM (1978) Ultrasonic wave and moduli changes in a curing epoxy resin. *Experimental Mechanics* 18(6): 227–232.
- Lionetto F and Maffezzoli A (2013) Monitoring the cure state of thermosetting resins by ultrasound. *Materials* 6(9): 3783–3804.
- Malaeb RA, Mahfoud EN and Harb MS (2018) Decomposition of fundamental Lamb wave modes in complex metal structures using COMSOL®. In: *COMSOL conference proceedings*, Lausanne, Switzerland, October 2018. Stockholm: COMSOL.
- Mehrabi M and Soorgee MH (2019) The use of ultrasonic guided waves in cure monitoring of adhesives. In: *The 9th international conference on acoustics and vibrations*, 24–25 December 2019. Tehran: ISAV.
- Mustapha S, Ye L, Wang D, et al. (2011) Assessment of debonding in sandwich CF/EP composite beams using A0 Lamb wave at low frequency. *Composite Structures* 93(2): 483–491.
- Nixdorf K and Busse G (2001) The dielectric properties of glass-fibre-reinforced epoxy resin during polymerisation. *Composites Science and Technology* 61(6): 889–894.
- Okabe Y, Fujibayashi K, Shimazaki M, et al. (2010) Delamination detection in composite laminates using dispersion change based on mode conversion of Lamb waves. *Smart Materials and Structures* 19(11): 115013.
- Pang KP and Gillham JK (1990) Competition between cure and thermal degradation in a high Tg epoxy system: Effect

- of time and temperature of isothermal cure on the glass transition temperature. *Journal of Applied Polymer Science* 39(4): 909–933.
- Prime RB (1970) Dynamic cure analysis of thermosetting polymers. In: Porter RS and Johnson JF (eds) *Analytical Calorimetry*. Boston, MA: Springer, pp.201–210.
- Scheerer M, Simon Z, Marischler M, et al. (2017) A Multifunctional piezo and temperature sensor for process and structural health monitoring of CFRP structures made by resin transfer molding. In: *9th European workshop on structural health monitoring (EWSHM)*, Manchester, UK, 10–13 July 2018. Northampton: BINDT.
- Stark W, Jaunich M and Mchugh J (2015) Dynamic Mechanical Analysis (DMA) of epoxy carbon-fibre prepregs partially cured in a discontinued autoclave analogue process. *Polymer Testing* 41: 140–148.
- Su Z, Ye L and Lu Y (2006) Guided Lamb waves for identification of damage in composite structures: A review. *Journal of Sound and Vibration* 295(3–5): 753–780.
- Vail J, Krick B, Marchman K, et al. (2011) Polytetrafluoroethylene (PTFE) fiber reinforced polyetheretherketone (PEEK) composites. *Wear* 270(11–12): 737–741.
- Vogelsang R, Brutsch R, Farr T, et al. (2002) Electrical tree propagation along barrier-interfaces in epoxy resin. In: *Annual report conference on electrical insulation and dielectric phenomena*, Cancun, Quintana Roo, Mexico, October 2002, pp.946–950. New York: IEEE.
- Wang J, Gangarao H, Liang R, et al. (2015) Durability and prediction models of fiber-reinforced polymer composites under various environmental conditions: A critical review. *Journal of Reinforced Plastics and Composites* 35(3): 179–211.